

2008

Growth of atomically flat nanofilms and surface superstructures of intrinsic liquid alloys

Toshiro Yamanaka

Jianli Wang

Tadaaki Nagao

Shin Yaginuma

Canhua Liu

See next page for additional authors

Follow this and additional works at: <https://ro.uow.edu.au/scipapers>



Part of the [Life Sciences Commons](#), [Physical Sciences and Mathematics Commons](#), and the [Social and Behavioral Sciences Commons](#)

Recommended Citation

Yamanaka, Toshiro; Wang, Jianli; Nagao, Tadaaki; Yaginuma, Shin; Liu, Canhua; Tupkalo, Andrey; and Sakurai, Toshio: Growth of atomically flat nanofilms and surface superstructures of intrinsic liquid alloys 2008.

<https://ro.uow.edu.au/scipapers/4927>

Growth of atomically flat nanofilms and surface superstructures of intrinsic liquid alloys

Abstract

Atomically flat nanofilms were formed during growth of Ga on a Si(111) surface using an In surfactant above the melting point of Ga (and In–Ga eutectic) throughout Ga coverages of 0.17 to 5 monolayers ($0.17 \leq \Theta_{\text{Ga}} \leq 5$). Unique superstructures such as a quasisquare-lattice (QS) structure at $\Theta_{\text{Ga}}=3$ to 4 and a 5x5 structure at $\Theta_{\text{Ga}}=5$ appeared as Θ_{Ga} increased. The QS structure had Ga dimer layers similar to the square lattices of an alpha-Ga(100) plane but also maintained the 1x1 structure of Si(111). As dimer layers transformed into a monoatomic layer, QS transformed into a 5x5 structure that no longer has square features.

Disciplines

Life Sciences | Physical Sciences and Mathematics | Social and Behavioral Sciences

Publication Details

Yamanaka, T., Wang, J., Nagao, T., Yaginuma, S., Liu, C., Tupkalo, A. V. & Sakurai, T. (2008). Growth of atomically flat nanofilms and surface superstructures of intrinsic liquid alloys. *Applied Physics Letters*, 92 (14), 143116-1-143116-3.

Authors

Toshiro Yamanaka, Jianli Wang, Tadaaki Nagao, Shin Yaginuma, Canhua Liu, Andrey Tupkalo, and Toshio Sakurai

Growth of atomically flat nanofilms and surface superstructures of intrinsic liquid alloys

Toshiro Yamanaka,^{1,a)} Jian-Li Wang,² Tadaaki Nagao,³ Shin Yaginuma,³ Canhua Liu,³ Andrey V. Tupkalo,² and Toshio Sakurai²

¹*Catalysis Research Center, Hokkaido University, Sapporo 001-0021, Japan*

²*Institute for Material Research, Tohoku University, Sendai, 980-8577, Japan*

³*Nano System Functionality Center, National Institute for Materials Science, 1-1 Namiki, Tsukuba 305-0044, Japan*

(Received 13 February 2008; accepted 20 March 2008; published online 11 April 2008)

Atomically flat nanofilms were formed during growth of Ga on a Si(111) surface using an In surfactant above the melting point of Ga (and In–Ga eutectic) throughout Ga coverages of 0.17 to 5 monolayers ($0.17 \leq \Theta_{\text{Ga}} \leq 5$). Unique superstructures such as a quasisquare-lattice (QS) structure at $\Theta_{\text{Ga}}=3$ to 4 and a 5×5 structure at $\Theta_{\text{Ga}}=5$ appeared as Θ_{Ga} increased. The QS structure had Ga dimer layers similar to the square lattices of an alpha-Ga(100) plane but also maintained the 1×1 structure of Si(111). As dimer layers transformed into a monoatomic layer, QS transformed into a 5×5 structure that no longer has square features. © 2008 American Institute of Physics. [DOI: 10.1063/1.2908930]

Growth of Ga on Si substrates is important not only as a fundamental science of liquid structures but also in relation to device technology of III–V semiconductors since the morphology of GaAs and GaN films is sensitively affected by the initial morphology of Ga films. For example, Ga grows into liquid droplets on semiconductor surfaces such as Si,^{1,2} GaAs,^{3,4} and GaN,⁵ which is usual growth of liquids. During exposure to As₄ or NH₃, the droplets react with As or N, resulting in the formation of GaAs and GaN nanodots with uniform sizes of several tens of nanometers.

In this letter, we describe the growth of Ga on Si(111)– $\sqrt{3} \times \sqrt{3}$ –In above the melting point of Ga. The initially adsorbed 1.3 monolayer (ML) of In acted as a surfactant^{6,7} segregating to the uppermost layer, resulting in abnormally flat films of Ga–In alloys that have never been observed in the growth of any metals or liquids. Unique two-dimensional (2D) ordered solid superstructures appeared depending on Ga coverages.

A Si(111)– 7×7 clean surface was made by annealing a Si(111) surface at 1250 °C for several minutes, and after about ten minutes, a Si(111)– $\sqrt{7} \times \sqrt{3}$ –In surface⁸ was prepared by deposition of In and brief postflashing to 300 °C for several seconds. After waiting for one hour for the surface to cool so as to stabilize the temperature and reduce the thermal drift during scanning tunnel microscope (STM) measurements, Ga was deposited on the surface before STM observation. The temperature of the surface during STM observation was above the melting point of Ga (29.8 °C) [and In–Ga eutectic (16 °C)] due to slow cooling rates of the sample and its holder. This was evidenced by the fact that STM images [Fig. 1(a)] and reflection high-energy electron diffraction patterns of pure Ga grown on a Si(111)– 7×7 surface showed droplets and halo rings, respectively, indicating a liquid structure of Ga. Hereafter, Θ_{Ga} is defined as number of MLs of Ga deposited with the atomic density of the Si(111) surface. Segregation of In to the uppermost layer was confirmed by Auger electron spectroscopy. The amount

of grown Ga was also monitored by Rutherford backscattering spectroscopy.

Figures 1(b) and 1(c) show large-scale STM images taken during the growth process. Nearly vertical steps (indicated by a large arrow) were always seen, and the terrace areas between these steps were atomically flat, though randomly distributed small holes (indicated by a small arrow) appeared as the extent of Ga coverage (Θ_{Ga}) increased. The shapes of steps became wavelike at high Θ_{Ga} , as shown in Fig. 1(c). However, the heights of these steps were always 3.1 Å regardless of Θ_{Ga} , and the distribution of the steps basically coincides with that of bilayer steps of the initial Si(111)– $\sqrt{7} \times \sqrt{3}$ –In surface. The height profile of a typical step at $\Theta_{\text{Ga}}=5$ [bottom of Fig. 1(c)] shows that the angle defined by θ_3 (15.8°) may be smaller (not zero) than the wetting angle of the Ga droplets [θ_1 (19.8°) and θ_2 (36.1°) in the profile in Fig. 1(a)]. It is surprising that no islands were observed on terraces at any value of Θ_{Ga} , even at $\Theta_{\text{Ga}} < 1$. These films are flatter than any other metal films⁹ and liquid films³ on semiconductor surfaces previously reported. The number and size of holes were small at small Θ_{Ga} but increased with increase in Θ_{Ga} . Figure 1(d) shows the distribution of depths of holes. The typical depth of holes at $\Theta_{\text{Ga}}=4$ is 3.9 Å, which decreased to about 2.7 Å at $\Theta_{\text{Ga}}=5$.

A variety of surface ordering patterns was observed during this growth process. At the initial stage, the areas of $\sqrt{7} \times \sqrt{3}$ structure decreased and a $3 \times \sqrt{3}/2$ structure appeared at $\Theta_{\text{Ga}}=0.5$. At $\Theta_{\text{Ga}}=1$, most of the areas exhibited a $\sqrt{3} \times \sqrt{3}$ structure. At $\Theta_{\text{Ga}}=2$ to $\Theta_{\text{Ga}}=3$, the $\sqrt{3} \times \sqrt{3}$ structure changed to quasisquare-lattice (QS) structures with longer periodicities. Figures 2(a) and 2(b) show STM images taken during the process of transformation from a $\sqrt{3} \times \sqrt{3}$ structure to a QS structure. The $\sqrt{3} \times \sqrt{3}$ structure and the QS structure tended to separately exist on different terraces, as shown in Fig. 2(a), but sometimes both of the structures existed on the same terrace, as shown in Fig. 2(b). At $\Theta_{\text{Ga}}=4$, most of the areas were covered by various domains of QS structures with some different orientations, as shown in Fig. 2(c). Distorted parallelogram lattices were often ob-

^{a)}Electronic mail: yama@cat.hokudai.ac.jp.

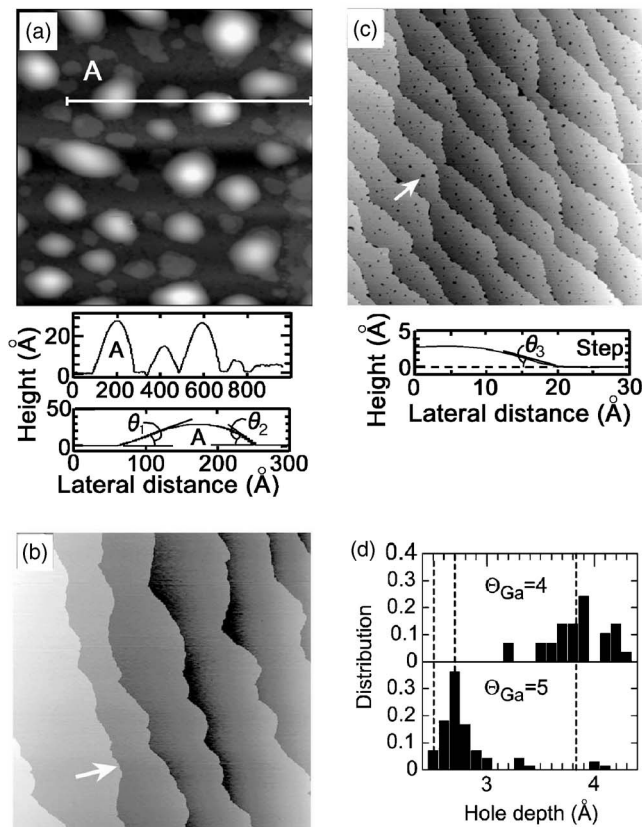


FIG. 1. Large-scale STM images of Ga grown (a) on Si(111)- 7×7 ($1200 \times 1200 \text{ \AA}$) and (b, c) on $\sqrt{7} \times \sqrt{3}$ -In ($1 \times 1 \mu\text{m}$) surfaces. (a) Sample bias (B_s) and tunnelling current (I_t) are -2.18 eV and 21.8 pA , respectively. (b) $\Theta_{\text{Ga}}=0.17$, $B_s=-1.43 \text{ eV}$, $I_t=14.8 \text{ pA}$. (c) $\Theta_{\text{Ga}}=5$, $B_s=-2.45 \text{ eV}$, $I_t=13.8 \text{ pA}$. Height profiles along the line in (a) and across a typical step at $\Theta_{\text{Ga}}=5$ are shown at the bottom of (a) and (c). Large and small arrows indicate a step and a hole, respectively. (d) Distribution of depths of holes at $\Theta_{\text{Ga}}=4$ and $\Theta_{\text{Ga}}=5$. Vertical dashed lines in (d) indicate the spacing between nearest atomic layers ($2.5\text{--}2.7 \text{ \AA}$) at liquid-vapor interfaces of Ga, In, and eutectic In:Ga alloy and the layer spacing (3.82 \AA) of α -Ga (001) planes that consist of upright Ga dimers.

served between two or three domains of QS structures, as shown in Fig. 2(d). High-resolution images taken within the area of Fig. 2(c) are shown in Figs. 2(e)–2(h). Figure 2(e) shows an image of the most frequently observed QS structure taken with a sample bias of -1.64 V . Fine lattices that correspond to a $\sqrt{3} \times \sqrt{3}$ structure are seen in addition to lattices of QS structures. However, with a lower sample bias of -417 mV , a STM image of the same area showed different fine lattices that correspond to a 1×1 structure, as shown in Fig. 2(f). Figure 2(g) shows a STM image of another area taken with a low sample bias of -171 mV . Fine lattices in this image correspond to a 1×1 structure in Fig. 2(f), but the directions of lattices of the QS structure are different from those in Fig. 2(f). Figure 2(h) shows the domain boundary between the two QS structures shown in Figs. 2(f) and 2(g). It can be seen that the fine 1×1 lattices are consistent across the domain boundary, while orientation of lattices of the QS structure changed. The variation in QS structure may be caused by local difference in surface concentration of In since the time scale of diffusion in this specific material may be very long because it has a large number of atoms in a unit cell, high degrees of freedom, and various quasistabilized structures (or since it is a premelted state). In fact, fuzzy features (scratcheslike feature) in Figs. 2(b) and 2(h) indicate

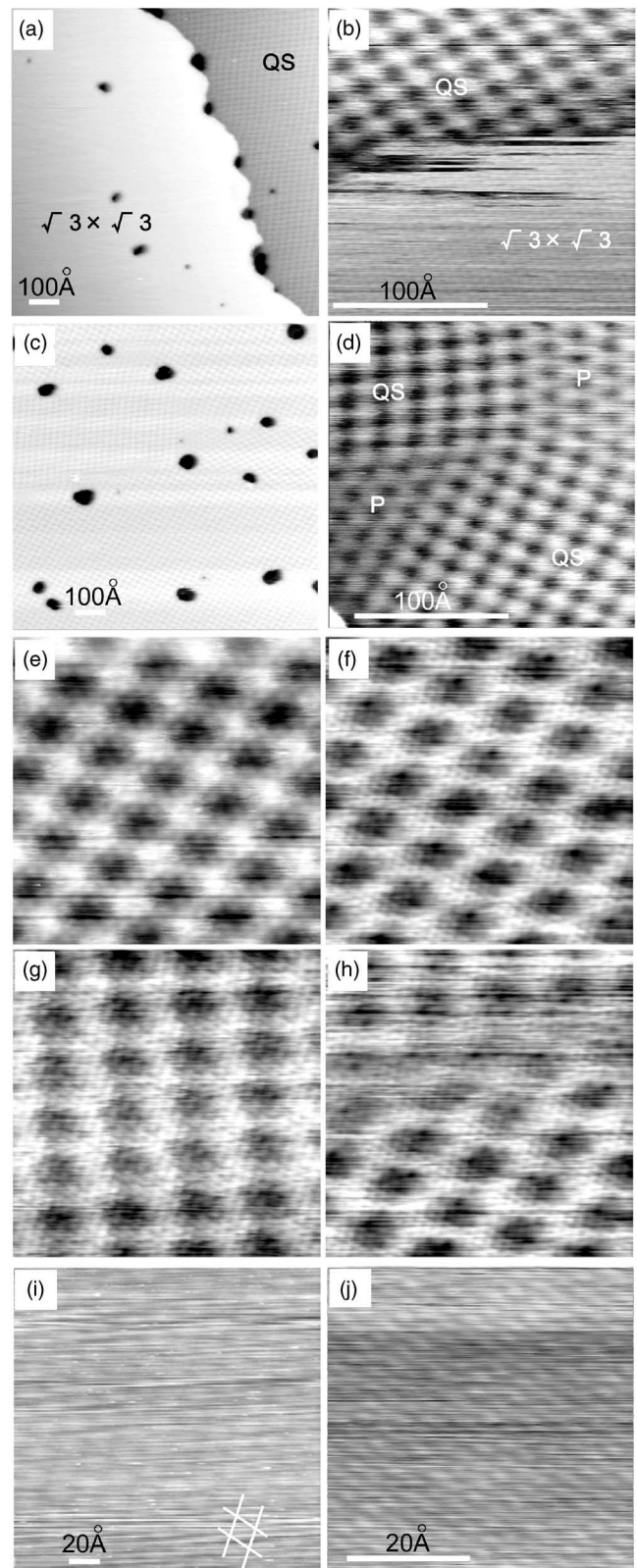


FIG. 2. (a)–(d) show large-scale STM images taken during growth of Ga on a Si(111)- $\sqrt{7} \times \sqrt{3}$ -In surface at $\Theta_{\text{Ga}}=2$ to $\Theta_{\text{Ga}}=4$. Scale bars indicate 100 \AA . (a) $\Theta_{\text{Ga}}=2$, $B_s=-1.56 \text{ V}$, $I_t=17.3 \text{ pA}$. (b) $\Theta_{\text{Ga}}=3$, $B_s=-1.55 \text{ eV}$, $I_t=19.9 \text{ pA}$. (c) $\Theta_{\text{Ga}}=4$, $B_s=-3.10 \text{ eV}$, $I_t=23.7 \text{ pA}$. (d) $\Theta_{\text{Ga}}=4$, $B_s=-2.70 \text{ eV}$, $I_t=11.9 \text{ pA}$. (e)–(h) show high-resolution ($100 \times 100 \text{ \AA}$) STM images of areas shown in Fig. 2(c) ($\Theta_{\text{Ga}}=4$). (e) $B_s=-1.64 \text{ V}$, $I_t=23.9 \text{ pA}$. (f) The same area as (e). $B_s=-417 \text{ mV}$, $I_t=20.4 \text{ pA}$. (g) $B_s=-171 \text{ mV}$, $I_t=17.7 \text{ pA}$. (h) A boundary between two domains of QS structures shown in (f) and (g). $B_s=-417 \text{ mV}$, $I_t=19.5 \text{ pA}$. (i) and (j) STM images taken at $\Theta_{\text{Ga}}=5$. Scale bars indicate 20 \AA . (i) $B_s=-257 \text{ mV}$, $I_t=18.3 \text{ pA}$. (j) $B_s=-337 \text{ mV}$, $I_t=23.5 \text{ pA}$. Lattices of 5×5 structures are shown by solid lines in (i).

that boundaries between different structures are still fluctuating.

At $\Theta_{\text{Ga}}=5$, the surface structure changed to a 5×5 structure [Fig. 2(i)] and fine 1×1 lattices were also observed [Fig. 2(j)]. A pair-correlation function obtained from Fig. 2(j) yielded a value of about 20 \AA for a decay length of ordering, which is longer than the general decay length (about three atomic diameters) of ordering in liquid metal, indicating the possibility of a crystalline structure of the outermost layer. The actual decay length may be longer than 20 \AA since the STM image represents only some of the atoms in the outermost layer in a small area. However, this outermost layer may be less ordered than usual crystalline since a decay length of $>100 \text{ \AA}$ was normally obtained from a STM image of Si(111)- 7×7 surfaces.

The initial substitution of In by Ga and wetting of Si(111) by Ga are consistent with a threshold temperature for desorption (i.e., binding energy) of Ga on Si(111) surfaces¹⁰ being higher than that of In.¹¹ During further growth of Ga, soluble In atoms diffuse into Ga, resulting in the formation of an outermost In ML.^{12,13} To change the morphology of grown Ga from droplets to a flat film, the surface energy of Si ($\sigma_{\text{Si}} \approx 1400 \text{ dyn/cm}$ at $30 \text{ }^\circ\text{C}$)¹⁴ must be larger than the sum of energy of the film surface σ_{fs} and energy of the Si-Ga interface $\sigma_{\text{Si-Ga}}$. Segregation of In should reduce σ_{fs} , since the surface energy of In [575 dyn/cm (unnaturally assuming that it is liquid at $30 \text{ }^\circ\text{C}$)¹⁵ and 650 dyn/cm (solid)¹⁶] is lower than that of Ga [718 dyn/cm (liquid at $30 \text{ }^\circ\text{C}$)¹⁵ and 800 dyn/cm (solid)¹⁶]. Probably, σ_{Si} and $\sigma_{\text{Si-Ga}}$ are also increased and decreased, respectively, by initial destruction of the Si(111)- 7×7 dimer adatom stacking fault structure¹⁷ that occurs during preparation of the $\sqrt{7} \times \sqrt{3}$ -In structure, and the condition of $\sigma_{\text{Si}} > \sigma_{\text{fs}} + \sigma_{\text{Si-Ga}}$ is attained. The non-zero value of θ_3 indicates that the superstructures are 2D ordered solid superstructures where kinetic limitations may prevent the layer from forming islands, since Ga will ball up in islands if the film is liquid.

The typical depth of holes at $\Theta_{\text{Ga}}=4$ [3.9 \AA , see Fig. 1(d)] is close to the layer spacing (3.82 \AA) of α -Ga(001) planes that consist of upright Ga dimers. Formation of α -Ga(001)-like layers was previously reported for the case of the interface between liquid Ga and a diamond (111) surface.¹⁸ Therefore, it is thought that Ga atoms formed upright dimers at $\Theta_{\text{Ga}}=4$ due to an effect of the solid-liquid interface. The QS structures may be induced by formation of

structures similar to square lattices of Ga dimers in α -Ga(001) planes. At $\Theta_{\text{Ga}}=5$, the QS structure suddenly disappeared, and the typical depth of holes decreased to about 2.7 \AA . This value is close to the distance between nearest neighbor atoms in bulk liquid Ga (2.56 \AA)¹⁹ and also the spacing between nearest atomic layers (2.5 – 2.7 \AA) at liquid-vapor interfaces of Ga,¹² In,²⁰ and eutectic In:Ga alloy,¹² suggesting formation of atomic layers with the 5×5 structure and no trace of the α -Ga(001) structure.

In summary, the formation of 2D ordered solid Ga is thought to be induced by the reduction of $\sigma_{\text{Si-Ga}}$ due to the destruction of the 7×7 structure, reduction of σ_{fs} due to surface segregation of In, and also the well-known effects of interface induced ordering.

We thank Professor T. Shikama for measurements of Rutherford back scattering spectroscopy. We also thank Dr. Y. Fujikawa and Dr. K. Wu for helpful discussion.

¹M. Shibata, S. S. Stoyanov, and M. Ichikawa, *Phys. Rev. B* **59**, 10289 (1999).

²K. Ueno, K. Saiki, and A. Koma, *Jpn. J. Appl. Phys., Part 1* **40**, 1888 (2001).

³N. Koguchi and K. Ishige, *Jpn. J. Appl. Phys., Part 1* **32**, 2052 (1993).

⁴T. Chikyow and N. Koguchi, *Jpn. J. Appl. Phys., Part 2* **29**, L2093 (1990).

⁵K. Kawasaki, D. Yamazaki, A. Kinoshita, H. Hirayama, K. Tsutsui, and Y. Aoyagi, *Appl. Phys. Lett.* **79**, 2243 (2001).

⁶M. Copel, M. C. Reuter, E. Kaxiras, and R. M. Tromp, *Phys. Rev. Lett.* **63**, 632 (1989).

⁷T. Yamanaka and S. Ino, *Phys. Rev. B* **66**, 153309 (2002).

⁸J. Kraft, M. G. Ramsey, and F. P. Netzer, *Phys. Rev. B* **55**, 5384 (1997).

⁹R. Koch, *J. Phys.: Condens. Matter* **6**, 9519 (1994).

¹⁰K. Fujita, Y. Kusumi, and M. Ichikawa, *Appl. Phys. Lett.* **68**, 631 (1996).

¹¹N. Minami, Y. Machida, T. Kajikawa, T. Sato, K. Ota, and S. Ino, *Surf. Sci.* **524**, 199 (2003).

¹²M. J. Regan, P. S. Pershan, O. M. Magnussen, B. M. Ocko, M. Deutsch, and L. E. Berman, *Phys. Rev. B* **55**, 15874 (1997).

¹³S. A. Rice and M. Zhao, *Phys. Rev. B* **57**, 13501 (1998).

¹⁴J. N. Israelachvili, *Intermolecular and Surface Forces*, 2nd ed. (Academic, London, 1991).

¹⁵T. Tanaka, M. Nakamoto, R. Oguni, J. Lee, and S. Hara, *Z. Metallkd.* **95**, 818 (2004).

¹⁶K. F. Wojciechowski, *Surf. Sci.* **437**, 285 (1999).

¹⁷K. Takayanagi, Y. Tanishiro, S. Takahashi, and M. Takahashi, *Surf. Sci.* **164**, 367 (1985).

¹⁸W. J. Huisman, J. F. Peters, M. J. Zwanenburg, S. A. deVries, T. E. Derry, D. Abernathy, and J. F. van der Veen, *Nature (London)* **390**, 379 (1997).

¹⁹A. H. Narten, *J. Chim. Phys. Phys.-Chim. Biol.* **56**, 1185 (1972).

²⁰H. Tostmann, E. DiMasi, P. S. Pershan, B. M. Ocko, O. G. Shpyrko, and M. Deutsch, *Phys. Rev. B* **59**, 783 (1999).